

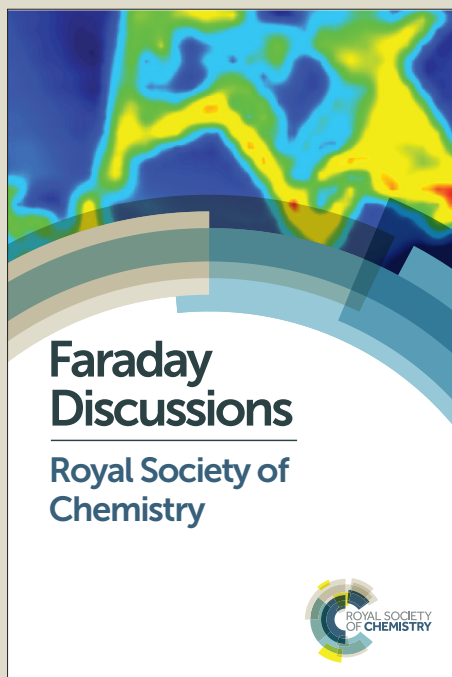
Faraday Discussions

Accepted Manuscript



This manuscript will be presented and discussed at a forthcoming Faraday Discussion meeting. All delegates can contribute to the discussion which will be included in the final volume.

Register now to attend! Full details of all upcoming meetings: <http://rsc.li/fd-upcoming-meetings>



This is an *Accepted Manuscript*, which has been through the Royal Society of Chemistry peer review process and has been accepted for publication.

Accepted Manuscripts are published online shortly after acceptance, before technical editing, formatting and proof reading. Using this free service, authors can make their results available to the community, in citable form, before we publish the edited article. We will replace this *Accepted Manuscript* with the edited and formatted *Advance Article* as soon as it is available.

You can find more information about *Accepted Manuscripts* in the [Information for Authors](#).

Please note that technical editing may introduce minor changes to the text and/or graphics, which may alter content. The journal's standard [Terms & Conditions](#) and the [Ethical guidelines](#) still apply. In no event shall the Royal Society of Chemistry be held responsible for any errors or omissions in this *Accepted Manuscript* or any consequences arising from the use of any information it contains.

This article can be cited before page numbers have been issued, to do this please use: L. Mohammadzadeh, P. Quaino and W. Schmickler, *Faraday Discuss.*, 2016, DOI: 10.1039/C6FD00076B.

Interactions of anions and cations in carbon nanotubes

L. Mohammadzadeh^{1,2}, P. Quaino², and W. Schmickler¹

¹ Institute of Theoretical Chemistry, Ulm University, Germany

² PRELINE, FIQ, Universidad Nacional del Litoral, Santa Fe, Argentina

April 12, 2016

Abstract

We consider the insertion of alkali-halide ion pairs into a narrow (5,5) carbon nanotube. In all cases considered, the insertion of a dimer is only slightly exothermic. While the image charge induced on the surface of the tube favors insertion, it simultaneously weakens the Coulomb attraction between the two ions. In addition, the anion experiences a sizable Pauli repulsion. For a one dimensional chain of NaCl embedded in the tube the most favorable position for the anion is at the center, and for the cation near the wall. The phonon spectrum of such chains shows both an acoustic and an optical branch.

1 Introduction

Carbon nanotubes hold great promises as electrode materials for batteries and supercapacitors: They have a high surface area, low weight, exist in semiconducting and conducting modifications, and can be doped by defects or impurities. They also pose a fundamental problem for double-layer theory: The dimensions of nanotubes, with diameters of the order of 1nm, are smaller than the characteristic lengths for double layers at planar surfaces. Hence the familiar concepts of double layer theory no longer apply, and new concepts are being called for. Given the small spatial extensions of nanotubes, any new model must be based on an atomistic description. Therefore, our group has embarked on a project to develop models for electrolytes in narrow tubes using a bottom-up approach, starting with single ions [1, 2, 3]. We use density functional theory (DFT) as a tool to explore the electronic properties of the system, and on this basis we construct physical models for the interaction of ions with nanotubes.

Our previous works in this area were devoted to single ions; here we go one step further and first consider ion pairs in nanotubes, and later a one-dimensional salt, i.e. a chain of anions and cations in alternating positions embedded in a tube. The central question is: How does the nanotube affect the interaction between the ions?

Throughout this work we focus on nanotubes with diameters of less than 1nm. This range is of particular interest, because such tubes have an unexpectedly high capacity [4, 5]. There is presently a debate, if the capacity per unit area of these tubes is actually higher than that of wider tubes – for a recent contribution to this question see [6]. A central difficulty is the measurement of the surface area of narrow tubes. However, the main point is that these narrow tubes have a high capacity, even though the ions have to lose a large part of their solvation shell when they enter the tube. The physical reason for this effect was pointed out by Kondrat and Kornyshev [7]: Ions in narrow tubes create an image charge on the adjacent walls, which lowers their energy and compensates for the loss of solvation energy. Further, the image charge effectively screens the Coulomb potential along the axis of the tube; this weakens the interaction between ions of the same sign, and allows a denser packing of charge. The same group has also developed two- and three-state Ising models for ionic liquids stored in carbon nanotubes (CNT) and calculated charge - capacity characteristics [8, 9, 10].

The rest of this article is organized as follows: In order to make this article self-contained we shall first briefly review a few results for the insertion of single ions. Then we shall present DFT results for a few ion pairs, which we shall interpret in terms a simple model. Next we shall examine a chain of NaCl as an example of a one-dimensional salt embedded in a tube, and finally calculate the phonon spectrum of such chains.

2 A few results for the insertion of single ions

In our previous works [1, 2, 3] we have investigated the insertion of simple alkali and halide atoms in a variety of CNTs, all with diameters less than 1 nm. In all cases investigated the inserted atoms were completely ionized, and did not form chemical bonds with the CNT. The charge that had been transferred to the CNT forms an image charge that surrounds the ion – see Fig. 1.

The energetics of ion insertion are governed by a competition between the image interaction and Pauli repulsion. The image interaction favors insertion and forms a large part of the total insertion energy; it is more favorable near the wall. In contrast, Pauli repulsion is weakest at the center. As a consequence, for larger ions, especially the halide ions, the optimum position in these narrow tubes is at

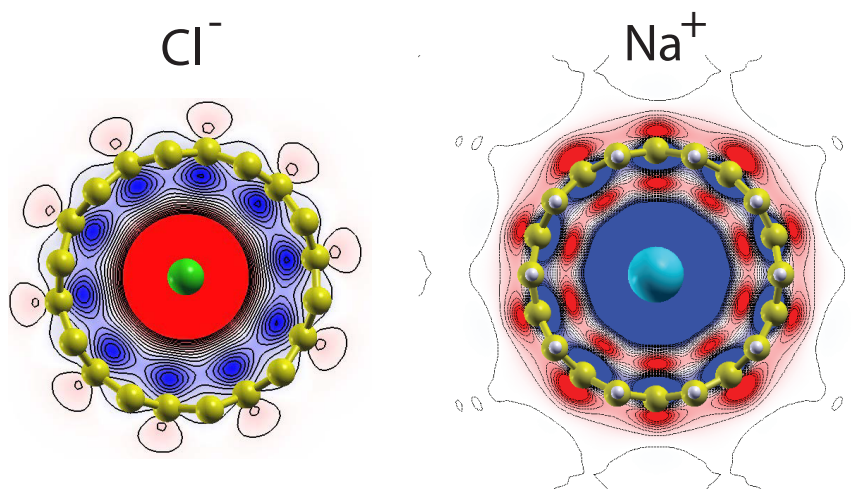


Figure 1: Charge difference plots for a chlorine and a sodium atom in a (10,0) CNT. Red (blue) indicates an excess of negative (positive) charge.

the center, while the smaller alkali ions Li^+ and Na^+ are usually incorporated off center.

Our calculations show that the image charge screens the Coulomb potential of the inserted ions and thus reduces the electrostatic interaction. This confirms the notion of a superionic state postulated by Kondrat and Kornyshev on the basis of classical electrostatics [7]. Figure 2 shows the screened Coulomb potential along the axis generated by a Li^+ ion for two CNTs with different properties: The (8,0)CNT is semiconducting and has a radius of 3.18 Å, while (6,3)CNT is conducting and has a very similar radius of 3.10 Å. In spite of their different conductivity, the two tubes show practically the same screening. In fact, the insertion of the Li atom has made the previously semiconducting (8,0)CNT conductive, because it has taken up an extra electron [3].

We have calculated the screened Coulomb potential for a series of alkali and halide ions; outside of the ionic core the potential is independent of the nature of the ion[1, 2]. This shows, that the screening is a purely electrostatic effect. In order to characterize the screening properties of a tube, we have introduced the notion of the *effective image radius of the tube*, which is the radius of a classical metal tube which produces the same screening as the real tube under consideration. For the two tubes shown in Fig. 2 the values are: $R_{\text{im}} = 2.14$ Å for the (8,0) CNT, and $R_{\text{im}} = 2.01$ Å for the (6,3) CNT. Thus, the effective image radius is smaller than the physical radius of the tubes as defined by the position of the carbon atoms. This confirms the visual impression of Fig. 1 that the image charge sits inside the

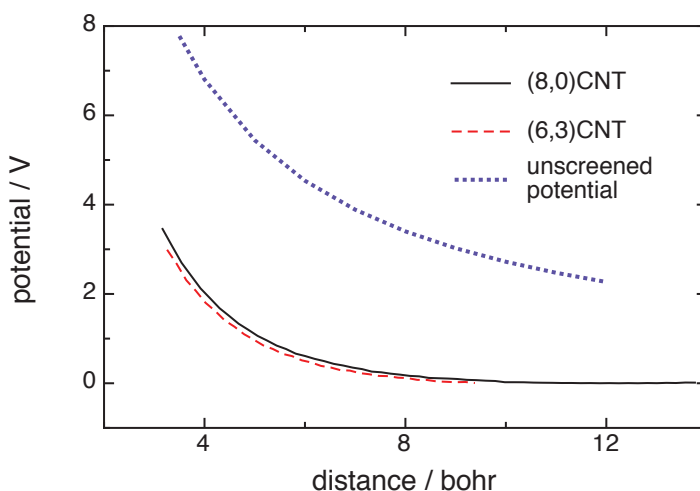


Figure 2: Electrostatic potential generated by a Li^+ ion along the axis of a (8,0)CNT and (6,3)CNT; the ion sits at the center of the tube. For comparison, we also show the unscreened Coulomb potential.

tube. We shall return to the concept of screening when we discuss the interaction between ion pairs.

3 Insertion of ion pairs

As a model tube we chose the (5,5)CNT, which is conductive and has a diameter of 6.78 Å. Note that in this paragraph we consider insertion into the center of the tube, because in this case the symmetry helps in understanding the energetics. Positions of the ions off center will be considered later. Figure 3 shows the pair NaCl inserted into the tube.

We inserted the ion pairs NaCl, LiCl, and LiF into this tube and calculated the equilibrium distances between the ions and the energetics of insertion by DFT. Table 1 gives the distances for the inserted pairs and compares them with the results of a model, described in the next section, with the bond distance of the diatomic molecule, and the bond distance of the corresponding salts, all of which have NaCl structure. In all cases the bond distance for the pair in the tube is somewhat larger than for the molecule. We ascribe this to the screening of the ionic charge, and will discuss this effect in greater detail below. In the salt the distance is even larger; this well known effect is caused by the repulsion from the six nearest neighbors.

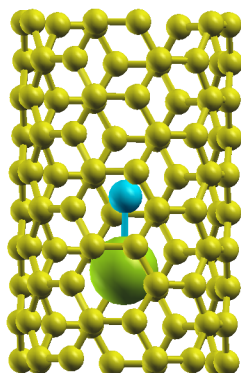


Figure 3: NaCl inserted into a (5,5)CNT; the small blue sphere indicates the position of Na^+ , the greenish sphere is Cl^- .

As usual we define the insertion energies of the ion pairs with respect to the atoms:

$$E_{\text{ins}}^{\text{atom}} = \text{energy}(\text{tube} + \text{ion pair}) - \text{energy}(\text{tube}) - \text{energy}(\text{alkali atom}) - \text{energy}(\text{halogen atom}) \quad (1)$$

Alternatively we can consider the insertion energy of the dimer:

$$E_{\text{ins}}^{\text{dimer}} = \text{energy}(\text{tube} + \text{ion pair}) - \text{energy}(\text{tube}) - \text{energy}(\text{dimer in vacuum}) \quad (2)$$

In both equations all subsystems considered are at equilibrium.

The insertion energies for the two atoms are quite favorable (see Tab. 2); they are almost equal for NaCl and LiCl, but much more favorable for LiF. Obviously, the Pauli repulsion, which is lower for F^- than for Cl^- , plays an important role. In contrast, the energy gained by inserting the dimer is quite low. The reason for this can be seen when we look at the binding energy E_{bind}^t for the pair inside the

pair	tube(DFT)	tube(model)	molecule	salt
NaCl	2.45	2.54	2.36	2.82
LiCl	2.07	2.15	2.02	2.57
LiF	1.60	1.63	1.56	2.01

Table 1: Equilibrium distances (in Å) for the ion pairs in the (5,5)CNT, the molecule and the salt; we also give the values calculated from a model described in the next section.

tube, i.e. the gain in energy when the two ions approach each other inside the tube from infinite separation to the equilibrium distance. This is much smaller than the formation energy in vacuum. As we shall explain in greater detail in the next section, this is caused by the screening of the charge by the image charge on the walls of the tube. In other words: what the ion pair gains in energy from the image charge, it loses in terms of binding energy.

To gain an impression of the screening we consider the charge redistribution caused by the insertion. Again there are two different ways to define them. The first is to refer them to the two inserted atoms:

$$\Delta\rho_1 = \rho(\text{tube} + \text{ion pair}) - \rho(\text{tube}) - \rho(\text{alkali atom}) - \rho(\text{halogen atom}) \quad (3)$$

Alternatively, it can be referred to the dimer in vacuum:

$$\Delta\rho_2 = \rho(\text{tube} + \text{ion pair}) - \rho(\text{tube}) - \rho(\text{dimer in vacuum}) \quad (4)$$

Both charge differences are shown in Fig. 4. The first quantity shows the ioniza-

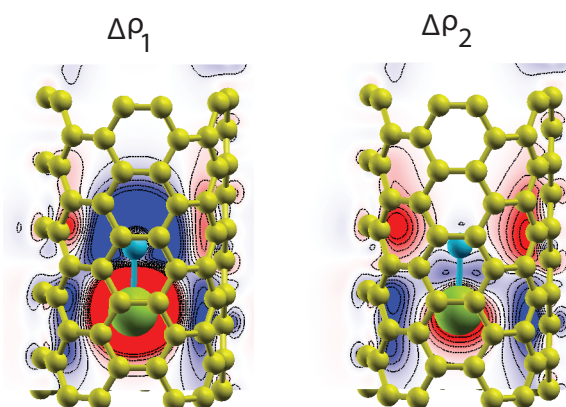


Figure 4: Charge differences for NaCl inserted into a (5,5)CNT; the small blue sphere indicates the position of Na⁺, the greenish sphere is Cl⁻. The l.h.s. refers to the insertion of the two atoms, the r.h.s. to the insertion of the dimer – see eqs. (3) and (4).

tion of the two atoms and the image charge; the latter shows the screening of the dimer more clearly.

It is of interest to compare the energies of insertion of the ion pairs with those of the individual ions. As we have argued before, for an infinite tube we can write the energy of insertion for an alkali atom as:

$$I_c = I_1 - \Phi + E_c \quad (5)$$

where I_1 is the first energy of ionization, Φ is the workfunction of the tube, and E_c is the interaction energy of the ion with the tube, which contains both the image energy and the Pauli repulsion. Likewise, for a halide atom we obtain:

$$I_a = -A + \Phi + E_a \quad (6)$$

where A is the electron affinity of the atom, and E_a the interaction energy of the anion with the tube. Taking the sum we obtain:

$$I_a + I_c = I_1 - A + (E_a + E_c) \quad (7)$$

where the work function has cancelled. For a finite system with relatively few free electrons, the energy required to take away an electron is not exactly equal to the energy gained by adding an electron; so eq. (7) is an approximation, which is useful to obtain the order of magnitude for the sum of the interaction terms ($E_a + E_c$), which is also given in Tab. 2. The values that we use here are for the center of the tube; this is the optimum position for the two anions considered, but not for the two cations. Therefore the repulsion energy should be determined by the anions, which is in line with the fact that ($E_a + E_c$) are almost equal for NaCl and LiCl, but is more favorable for LiF with the smaller anion.

For comparison we note that the image energy of a univalent ion at the center of the tube is:

$$E_{\text{im}} \approx \frac{-0.436}{R_{\text{im}}} \quad \text{in a.u.} \quad (8)$$

where R_{im} is the effective image radius of the tube, which in this case is $R_{\text{im}} = 3.8$ (a.u.) ≈ 2 Å, so that $E_{\text{im}} \approx -3.12$ eV. In all cases $|(E_a + E_c)|$ is much smaller than $|2E_{\text{im}}|$, so the effect of Pauli repulsion is considerable.

pair	$E_{\text{ins}}^{\text{atom}}$	$E_{\text{ins}}^{\text{dimer}}$	E_{mol}	E_{bind}^t	$E_a + E_c$	E_t
NaCl	-4.43	-0.22	-4.211	-1.36	-2.65	-4.01
LiCl	-4.96	-0.14	-4.82	-2.07	-2.73	-4.80
LiF	-6.60	-0.65	-5.95	-2.71	-3.73	-6.44

Table 2: Various energies associated with the insertion of ion pairs: $E_{\text{ins}}^{\text{atom}}$ is the insertion energy referred to the insertion of the two atoms as defined by eq. (1); $E_{\text{ins}}^{\text{dimer}}$ is the insertion energy referred to the insertion of the dimer as defined by eq. (2); E_{mol} is the binding energy of the binary molecule in the vacuum; E_{bind}^t is the binding energy of the pair in the tube. E_a and E_c are the insertion energies for a single anion or cation. $E_t = E_a + E_c + E_{\text{bind}}^t$, and should roughly equal the insertion energy $E_{\text{ins}}^{\text{atom}}$.

The sum ($E_a + E_c$) refers to the insertion of two individual, non-interacting ions. To a first approximation, it should differ from the insertion energy of the ion pair by the binding energy E_{bind}^t for the pair in the tube:

$$E_t = E_a + E_c + E_{\text{bind}}^t \approx E_{\text{ins}}^{\text{atom}} \quad (9)$$

As can be seen from the last column in Tab. 2, this relation holds to first order. Deviations are caused by the fact, that Pauli repulsion deforms also the electronic structure of the tube, which in turn effect the work function – in other words, the various interactions are not strictly additive. Therefore the deviation is greatest for NaCl, the largest pair of ions.

4 Extension of the Rittner model

Alkali halide molecules are good model systems for understanding ionic bonds. Therefore, they were a popular topic of research before the advent of computer chemistry, and several models have been constructed for their binding properties. The simplest model contains only the Coulomb attraction and a repulsive term [11], but better versions include terms for the ion-induced dipole interactions and a van der Waals term. A good parametrization of the latter kind of model has been proposed by Rittner [12], where the interaction potential is written in the form:

$$V(R) = -\frac{1}{R} - \frac{(\alpha_1 + \alpha_2)}{2R^4} - \frac{2\alpha_1\alpha_2}{R^7} + A \exp -\frac{R}{\rho} - \frac{C}{R^6} \quad (10)$$

Here, R is the separation between the two ions, α_1 and α_2 are their polarizabilities, and A and ρ are constants; atomic units have been used. The meaning of the individual terms is as follows: (1) Coulomb attraction; (2) and (3): ion-induced dipole interaction; (4) Pauli repulsion, and (5) van der Waals attraction. Within a nanotube the Coulomb attraction is strongly screened [7], so that the first term must be adapted to the new surroundings. The charge on the ions gives rise to a compensating image charge on the walls of the tube. As we have discussed above, the resulting screened potential can be described by an effective image radius R_{im} , which has the following interpretation: The screened Coulomb potential is the same as that produced by a classical metal tube of radius R_{im} . Considering ions along the center of the tube, this potential can be written as:

$$\Phi(z) = \frac{2}{R} \sum_{m=1}^{\infty} \frac{\exp(-k_m z/R)}{k_m |J_1(k_m)|^2} \quad (11)$$

where z is the distance from the center of the ion, k_m denotes the roots of the Bessel function $J_0(k_m) = 0$, and J_1 is the Bessel function of first order. This formula is easily programmed, and we have used it here. It is, however, not very

practical for computer simulations, and therefore it is sometimes approximated by the first and leading term – see e.g. [13] – at larger distances. However, a better and even simpler approximation is to spread the image charge uniformly on an infinitely thin ring surrounding the ion:

$$\Phi(z) \approx \frac{1}{z} - \frac{1}{\sqrt{z^2 + R^2}} \quad \text{for large } z \quad (12)$$

In order to test if the concept of screening can be applied to the ion pairs in CNTs, we have replaced the first term in eq.(10) by $-\Phi(R)$ as given by eq. (11). For explicit calculations we have taken the parameters for the various ions from [14]; for the effective image radius of the (5,5)CNT we have used the value of $R_{\text{im}} = 2.0$ Å determined in [2]. In this way we have calculated the potential energy curves

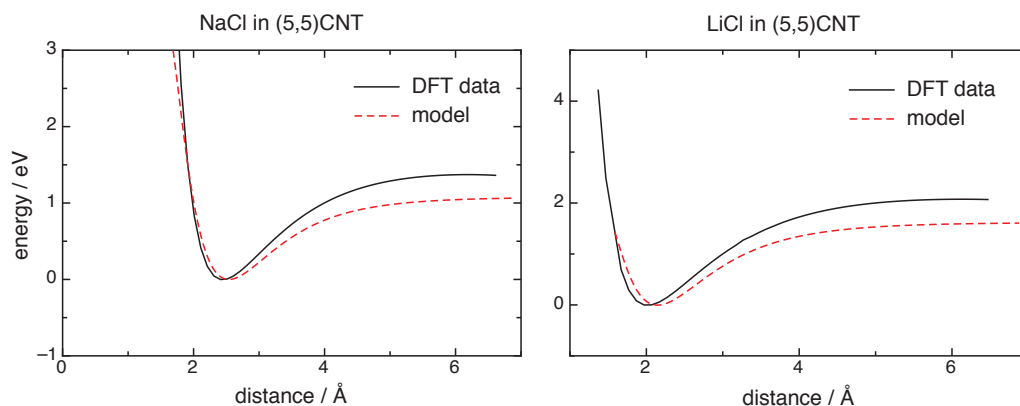


Figure 5: Potential energy curves for the ion pairs in a (5,5)CNT; the energy at the minimum has been set to zero.

for NaCl and LiCl in the nanotube; the results are shown in Fig. 5, where they are compared with the results from DFT calculations. Near the minima the two curves agree quite well; in particular the bond distance is well represented – see also Tab. 1. At larger distances the agreement is not so good, and the binding energies are too low by a few tenths of an eV. We surmise that this discrepancy is caused by the ion-induced dipole terms in eq. (10), which are based on the assumption that the ion potential is unscreened. We have refrained from introducing corrections, because the original values from ref. [14] are semiempirical. In any case the model calculations explain the great reduction in binding energy from the molecule in vacuum (-4.211 eV for NaCl and -4.82 eV for LiCl) caused by the screening.

5 One-dimensional NaCl

Up to now we have considered only ions positioned in the center of the tube; this greatly helped in the interpretation of the results, and allowed the application of simple models. The center is indeed the optimum position for the anions considered [3], but not for small cations like Li^+ and Na^+ , which prefer to reside near the wall. So in this section we shall study a truly one-dimensional chain of NaCl in our tube, and investigate two configurations: (1) all ions lined up along the axis; (2) all ions at their optimum position; the latter gives rise to a zig-zag configuration, in which the anion is at the center and the cation at the side. The corresponding arrangements are shown in Fig. 6.

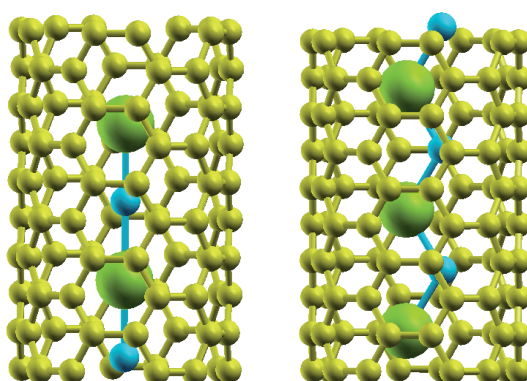


Figure 6: One-dimensional NaCl chain; linear configuration in the center of the tube (left), and zig-zag configuration in the equilibrium position (right)

In order to compare the insertion energies for the chains with those for the ion pairs we define:

$$\Delta E = [\text{energy}(\text{tube} + \text{chain}) - \text{energy}(\text{tube})] \quad (13)$$

$$- m \text{energy}(\text{Na}) - m \text{energy}(\text{Cl})/m \quad (14)$$

where m is the number of ion pairs per unit cell. As expected, the zig-zag configuration is more stable than the linear, but the difference is quite small. In both cases the insertion energy is more favorable than for the ion pair, where it is -4.01 eV. This is understandable, because here each ion has two neighbors. If the interaction of an ion with its two neighbors were additive, ΔE would be equal to the sum of the insertion energy plus the ion formation energy E_{tube}^t inside the tube, which is $-4.01 - 1.36$ eV = -5.37 eV. In fact, the binding is somewhat less favorable.

For the zigzag geometry the bond distance is slightly smaller than for the ion pair, where it is 3.45 Å. In contrast, in the linear geometry it is slightly larger, and it varies between the ion pairs, because the positions of the ions are not equivalent. In all cases the bond distance is larger than that for a molecule in vacuum and smaller than that for the three-dimensional salt (see Tab. 1).

Such one-dimensional salts embedded in a CNT have indeed been observed experimentally: Senga et al. [15] have formed a 1-D chain of CsI in a double-walled nanotube and imaged the system with a high-resolution transmission electron microscope. They accompanied their experimental work by DFT calculations. Their results are quite compatible with ours: They observed a binding distance of about 3.4 Å, a little larger than the value for the CsI molecule in vacuum (3.3 Å), and smaller than for the CsI crystal. Their calculations indicate that the anion is fixed at the center, while the cation can move more freely in the axial direction. In this context the earlier work of Fan et al. [16] on a chain of iodine atoms embedded in a CNT is also of interest. They observed that the optimum position of iodine is near the wall, and the chains had a helical structure. These nanotubes had a diameter 13.6 Å and were thus wider than those studied by Senga et al. and by us. So there is no contradiction. As we have pointed out before [3], for sufficiently wide tubes the optimum position must always be near the wall. Finally we mention that in earlier works by Green et al. [17, 18] the chains embedded in CNTs were still a few atoms wide.

6 Phonon spectrum

In a recent communication one of us [19] has considered the capacity of a nanotube permeable to only one kind of ion. In this context, he also considered the phonon spectrum of the vibrations along the axis of the tube. Because of the screening of the Coulomb force it was sufficient to consider the interaction between nearest neighbors only. The problem then reduces to a textbook problem and the resulting spectrum consists of one acoustic branch. In our case the spectrum is more interesting, since we have two kinds of ions with different masses. Specifically we consider a one-dimensional salt consisting of a chain of two kinds

geometry	$d / \text{Å}$	$\Delta E / \text{eV}$
zigzag	2.40	-4.94
linear	2.53 - 2.62	-4.87

Table 3: Bond distances and insertion energies for zigzag and linear geometry

of ions aligned along the axis of the tube. The equations of motions for the ions can be written in the form:

$$m_1 \frac{d^2 s_n^{(1)}}{dt^2} = -f \left(s_n^{(1)} - s_n^{(2)} - s_{n-1}^{(2)} \right) \quad (15)$$

$$m_2 \frac{d^2 s_n^{(2)}}{dt^2} = -f \left(s_n^{(2)} - s_n^{(1)} - s_{n+1}^{(1)} \right) \quad (16)$$

where the superscripts (1) and (2) refer to the two kinds of ions, s denotes a deviation from the equilibrium position, m a mass, and f is the force constant. Again, this is a textbook problem that is treated on a number of webpages –see e.g. [20]. The spectrum now has two branches given by:

$$\omega_{\pm}^2 = \frac{f}{\tilde{m}} \pm f \sqrt{\frac{1}{\tilde{m}^2} - \frac{4}{m_1 m_2} \sin^2 \left(\frac{ka}{2} \right)} \quad (17)$$

where \tilde{m} is the reduced mass, a the lattice constant and k the wave vector. Because

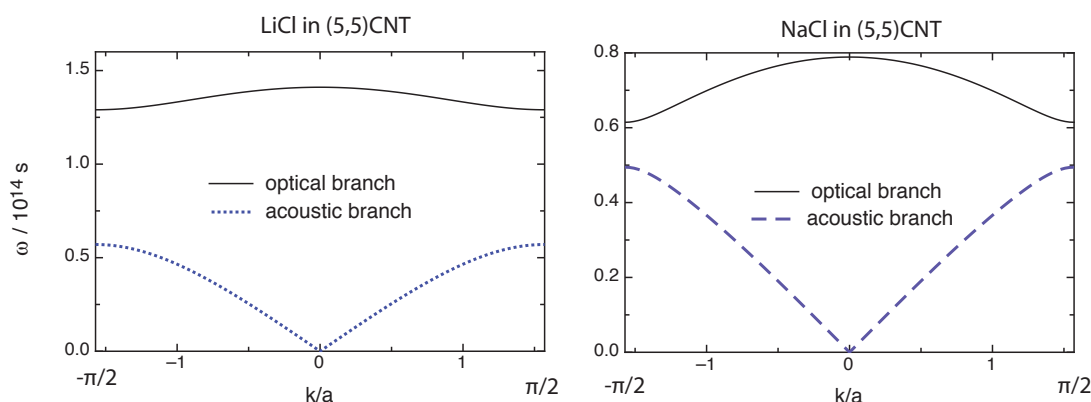


Figure 7: Phonon spectra for LiCl and NaCl.

of the different masses of the two ions the spectrum now has an acoustic branch, which corresponds to the minus sign in eq. (17), and an optical branch corresponding to the plus sign. Figure 7 shows the spectra for LiCl and NaCl, aligned along the center of the tube, as examples. Since the lithium ion has a smaller mass, the frequencies are higher for LiCl than for NaCl. Such phonon spectra have been measured for thin films of salts [21], but not yet for one-dimensional salts.

7 Conclusions

In this work we have considered the simultaneous insertion of an alkali and a halide atom into a narrow (5,5)CNT. The energies gained by inserting two individual atoms are quite high, of the order of several eV. However, the gain by inserting the alkali-halide dimer from the vacuum is quite small, less than one eV. One of the reasons is the Pauli repulsion, which in particular the larger halide ions experience. In addition, the image charge formed on the wall of the tube has two contrary effects: The interaction of the ions with the image charge favors insertion, but on the other hand it weakens the binding between the two ions.

The same principles govern the formation of a one-dimensional salt embedded in the tube. In particular, we have studied two configurations for the NaCl chain: aligned along the center, and the optimum configuration in which the cation is displaced towards the wall. The energy difference between these configurations is quite small, indicating that the cation has some freedom to move radially. The phonon spectrum of such 1D-salts shows both an acoustic and an optical branch.

Acknowledgements

Financial support by the Deutsche Forschungsgemeinschaft under Schm344/48-1 is gratefully acknowledged. We also thank the DAAD-DAHZ for funding the exchange between Ulm University and the Universidad del Litoral, Santa Fe. P.Q. thanks PICT-2014-1084, CONICET, UNL and Santa Fe Science Technology and Innovation Agency (ASACTEI, grant 00010-18-2014) for continuous support. W.S. thanks CONICET for continuous support.

Technical details of the DFT calculation

The DFT calculations have been performed in the same way as in [3]. We briefly summarize the main points. The correlation and exchange functionals were described within the generalized gradient approximation (GGA) in the Perdew, Burke and Ernzerhof (PBE) flavor [22]. The electron-ion interactions were represented through ultrasoft pseudopotentials [23], and a plane wave basis set was used to describe the valence electrons. The basis set was expanded to a kinetic energy cutoff of 400 eV (450 eV for the density). Brillouin zone integration was performed using the Gamma point. The carbon nanotubes were studied by using VASP [24] code. Periodic boundary conditions were used in order to correctly represent the infinite nanotubes. A separation of 15 Å between neighboring systems was imposed in the directions perpendicular to the tubes and in order to avoid in-

interactions between neighbor images. All the nanotubes and alkali or halide atoms were fully relaxed until the total forces were less than 40 meV/Å. All the systems used were neutral, but we confirmed the loss or gain of charge in the central atom by using Bader analysis method [25]. We used a dipole-correction scheme [26] in the systems that are not completely symmetric, in order to have a well-defined vacuum potential. The electrostatic part (ionic and Hartree potentials) of the local potential was calculated, but the exchange-correlation was not added.

References

- [1] A. Goduljan, F. Juarez, L. Mohammadzadeh, P. Quaino, E. Santos, and W. Schmickler, *Electrochem. Comm.* **45** (2014) 48.
- [2] Leila Mohammadzadeh, Aleksej Goduljan, Fernanda Juarez, P. Quaino, E. Santos, and W. Schmickler, *Electrochim. Acta*, **162** (2015) 11.
- [3] Leila Mohammadzadeh, Aleksej Goduljan, Fernanda Juarez, Paola Quaino, Elizabeth Santos, and Wolfgang Schmickler, *ChemPhysChem*, **17** (2016) 78.
- [4] J. Chmiola, G. Yushin, Y. Gogotsi, C. Portet, P. Simon, and P. Taberna, L. 2006 Anomalous increase in carbon capacitance at pore sizes less than one nanometer *Science* **313** (2006) 1760.
- [5] C. Largeot, C. Portet, J. Chmiola, P-L. Taberna, Y. Gogotsi, and P. Simon, *J. Am. Chem. Soc.* **130** (2008) 2730.
- [6] N. Jäckel, M. Rodner, A. Schreiber, J. Jeongwook, M. Zeiger, M. Aslan, D. Weingarh, and V. Presser, *J. Power Sources*, in press, <http://dx.doi.org.10.1016/j.jpowsour.2016.003.015>.
- [7] S. Kondrat and A. Kornyshev, *J. Phys.: Condens. Matter* **23** (2011) 022201.
- [8] A. Lee, S. Kondrat, and A. Kornyshev, *Phys. Rev. Lett.* **113** (2014) 048701.
- [9] A. Kornyshev, *Farad. Disc.* **164** (2013) 117.
- [10] C. Rochester, A. Lee, G. Pruessner, A. Kornyshev, *ChemPhysChem* **14** (2013) 4121.
- [11] N.W. Ashcroft and N.D. Mermin, *Solid State Physics*, Saunders College, Philadelphia, 1976.
- [12] E.S. Rittner, *J. Chem. Phys.* **19** (1951) 1030.

- [13] A. Kornyshev, *Faraday Discuss.*, **164** (2013) 117.
- [14] T. Gowda and S. Benson, *J. Phys. Chem.* **86** (1982) 847.
- [15] R. Senga, H.-P. Komsa, Zheng Liu, K.i Hirose-Takai, A. V. Krasheninnikov and K- Suenaga. *Nature Mat.* **13** (2014) 1050.
- [16] X. Fan, E. C. Dickey, P. C. Eklund, K. A. Williams, L. Grigorian, R. Buczko, S.T. Pantelides, and S.J. Pennycook, *Phys. Rev. Lett.* **84** (2000) 4621.
- [17] R. R. Meyer, J. Sloan, R. E. Dunin-Borkowski, A. I. Kirkland, M. C. Novotny, S. R. Bailey, J. L. Hutchison, and M. L. H. Green. *Science*, **289** (2002)1324.
- [18] J. Sloan A. I. Kirkland J. L. Hutchison M. L .H. Green. *Chem. Commun.*, page 1319, (2002).
- [19] W. Schmickler, *Electrochim. Acta.* **2015** 173 91.
- [20] www.itp.tu-berlin.de/fileadmin/a3233/upload/SS12/TheoFest2012/Kapitel/Chapter7.pdf
- [21] T.G. Fiske and L.B. Coleman, *Phys. Rev. B* **45** (1992) 1414.
- [22] J.P. Perdew, K. Burke, M. Ernzerhof, *Phys. Rev. Lett.* **1996**, 77, 3865.
- [23] D. Vanderbilt, *Phys. Rev. B* **1990**, 41, 7892.
- [24] (a) G. Kresse, and J. Hafner, *Phys. Rev. B* **1993**, 47, 558. (b) G. Kresse, and J. Hafner, *Phys. Rev. B*, **1994**, 49, 14251.
- [25] (a) R.F.W. Bader, P.E. Cade, P.M. Beddall, *J. Am. Chem. Soc.*, **1971**, 93, 3095. (b) G. Henkelman, A. Arnaldsson, H. Jonsson, *Comput. Mater. Sci.* **2006**, 36, 354.
- [26] L. Bengtsson, *Phys. Rev. B* **1999**, 59, 12301.